CHAPTER 3

Mechanisms of Copper Oxide Nanostructure Formation by Microwave-assisted Thermal Oxidation

This chapter presents the formation mechanism of copper oxide nanofibers and copper oxide nanoparticles under rapid microwave radiation as shown in Figure 3.1.

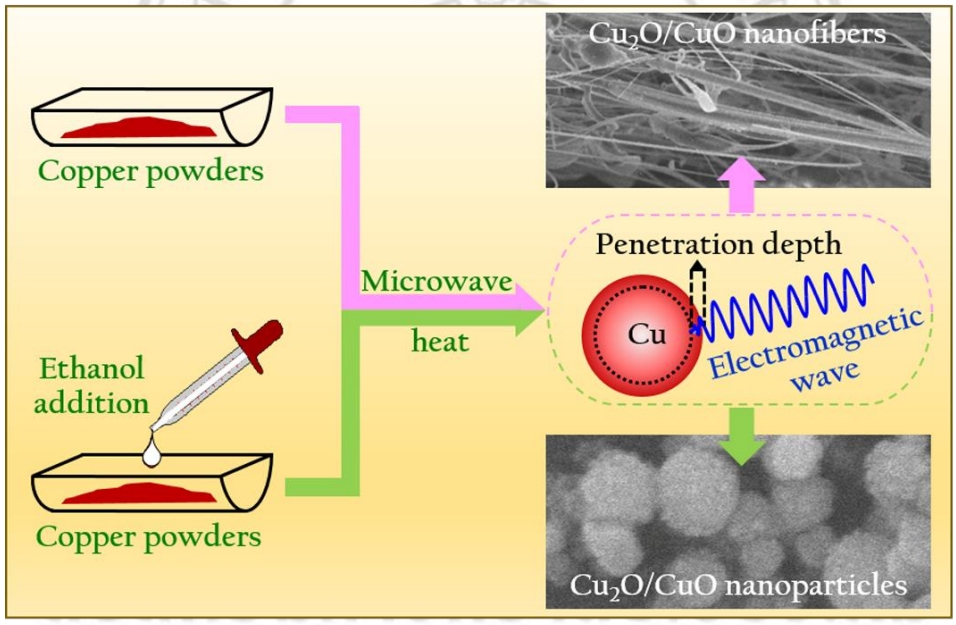

Figure 3.1 Schematic of copper powders and copper powder-ethanol interactions under microwave radiation leading to morphological formation of mixed-phase copper oxide nanofibers and nanoparticles, respectively.

The rapid syntheses of copper oxide nanostructures in two different forms were set up using microwave-assisted hybrid heating. Copper oxide nanofibers were initially synthesized by using only 1 g copper powders (99.5%, MW: 63.55g/mol, 40 μm of particle size) as a precursor and placing them in a quartz tube. This tube was then placed in a microwave, which had been punctured in two spots, and heated at 700 Watt for 7 min, in air without the need for an inert protective atmosphere. Next, copper oxide

nanoparticles were synthesized under the same conditions as the fibers except various amounts (0-0.4 mL) of ethanol were added into the precursor.

The formation mechanisms of the both morphologies were presented in four processes, microwave absorption, plasma phenomena, nucleation and structure formation as shown in Figure 3.2.

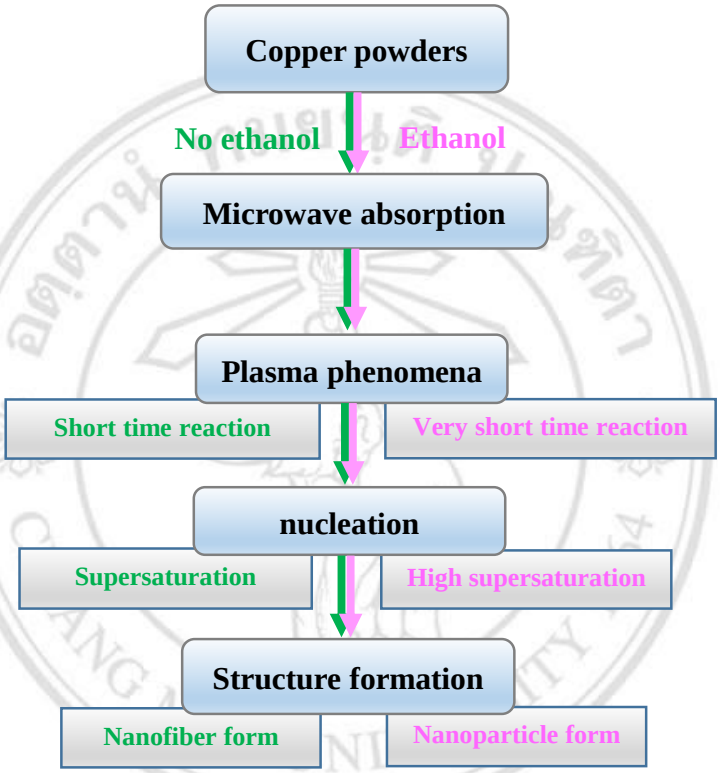

Figure 3.2 The flow chart of formation mechanism of copper oxide nanostructures synthesized by microwave-assisted thermal oxidation.

3.1 Microwave Absorption

Microwave energies were directly delivered to copper powder materials through molecular interaction with the electromagnetic field. The copper powders absorbed microwaves when they were heated in microwave fields in normal atmosphere as shown in Figure 3.3 (a, b). As travelling electromagnetic waves were transmitted into the surface of the metal Cu particles (40 μm in size), microwave energy (2.45 GHz, $\lambda \approx 12.24$ cm) was instantaneously absorbed and stored within a specific surface penetration of the Cu particles. The specific surface penetration depth is a shell having the thickness equal to the skin depth (d) at which the magnitude of the field strength reduces to 1/e or 36.8%

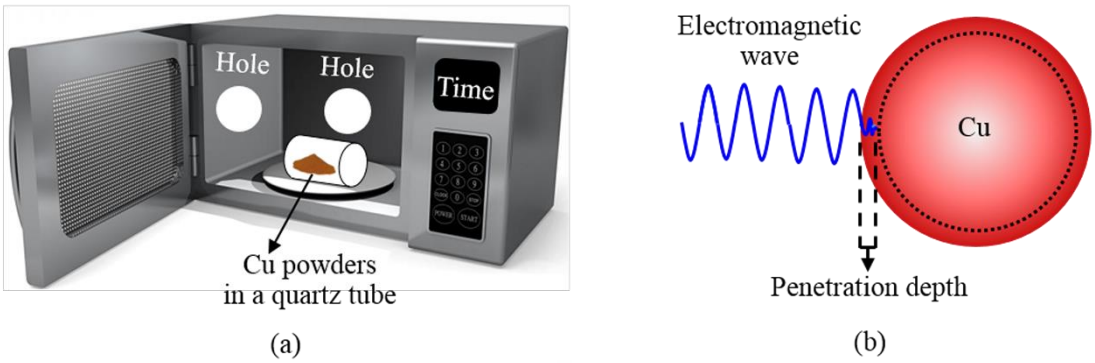

Figure 3.3 Schematic of (a) microwave-assisted synthesis of copper oxide nanostructures and (b) Cu particle-microwave absorption showing volumetric penetration depth.

of its value at a distance of one skin depth [91].

Skin depths of the various metals are limited in the range of a few microns, depending on the frequency of microwaves including also the permittivity and permeability of matter as follows [92]

$$d = \frac{1}{\alpha}, \tag{3.1}$$

where α is the attenuation factor and can be represented as

$$\alpha = \omega\sqrt{\frac{\mu_0\mu'\varepsilon_0\varepsilon'}{2}}\sqrt{\left[1+\left(\varepsilon''_{eff}\ /\ \varepsilon'\right)^2\right]^{1/2} - 1}. \tag{3.2}$$

Here, ω is the angular frequency of microwaves, μ_0 is the absolute permeability of free space ($4\pi\times10^{-7}$ H/m), μ' is the magnetic permeability, ε_0 is the absolute permittivity of free space (8.85×10^{-12} F/m), ε''_{eff} is the effective relative dielectric loss factor due to the ability of the material to store energy under the influence of an alternating electric field, and ε' is relative dielectric constant representing the penetration of microwaves into the material. The loss tangent, $\tan\delta$, represents the efficiency of the material to convert absorbed energy as seen in the following equation: [93]

$$\tan\delta = \frac{\varepsilon''_{eff}}{\varepsilon'}, \tag{3.3}$$

where δ is a phase lag. This presents the phase difference between the oscillating electric field of microwaves and the polarization of the material. For a conductor which has a high dielectric loss, $\varepsilon''_{polarization} = 0$, $\varepsilon''_{eff} / \varepsilon' >> 1$, the penetration depth approaches zero. Conductors with this dielectric behavior are considered to be as reflectors. Then, for $\mu' \sim 1$, the penetration depth depends only on frequency of operation, permeability and conductivity of a conductor as follows [92] (Deriving physics equations is shown in APPENDIX B).

$$d = \sqrt{\frac{1}{\sigma\pi f \mu_0}}, \tag{3.4}$$

where $\sigma = \omega\varepsilon_0\varepsilon''_{eff}$ is the dc electrical conductivity of a conductor and f is the microwave frequency. According to Eq. (3.3), skin depth of bulk copper is about 1.33 μm. Pure copper powders with diameters of a few microns to hundreds of microns in size can generate heat rapidly in a microwave [94]. Because the particle size (Cu~40 μm) is much smaller than the microwave wavelength (λ~12.24 cm), the electromagnetic field across the particle is uniform causing volumetric heating. The electromagnetic power absorbed per unit volume by powder particles can be written as [95]

$$P_{EM} = \omega \left\{ \begin{matrix} \varepsilon_0 \varepsilon''_{eff} \left| E_{rms} \right|^2 \\ +\mu_0 \mu''_{eff} \left| H_{rms} \right|^2 \end{matrix} \right\}, \tag{3.5}$$

where μ''_{eff} is the effective relative magnetic loss factor, E_{rms} and H_{rms} are root-mean-square values of electric field and magnetic field amplitudes, respectively. As a result, the Cu particles interacted with both the magnetic and electric fields of the microwave.

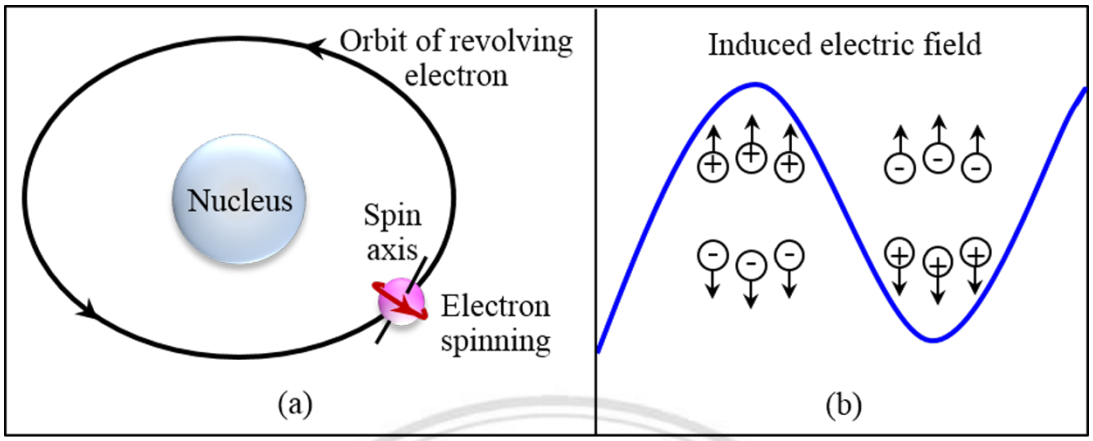

Figure 3.4 Schematic of (a) revolving and spinning electron of Cu atom and (b) induced electric field at Cu surface by a charge motion under microwave radiation.

However, the Cu particles weakly responded to the force of the magnetic field because Cu is a diamagnetic material. Diamagnetic materials are balanced in atomic magnetic effects, so the net magnetic moment per atom is zero. Thus, the Cu atoms induced a weak magnetic field in the opposite direction of the external magnetic field by orbiting and spinning electrons as shown in Figure 3.4 (a). This leads to the creation of extremely small current loops at the surfaces [96, 97]. In the meantime, the electric field is significantly enhanced at the surface of the material. All Cu atoms responded to an external electric field causing a charge motion and causing them to orient themselves with the field as shown in Figure 3.4 (b). This phenomena, which can result in dielectric loss, is called polarization [92, 97] (Definition is shown in APPENDIX C). However, the dielectric and magnetic losses caused little heat in the Cu particles. Therefore, the main cause of localized overheating in Cu particles occurred from conduction loss. Since some parts of the microwaves were absorbed and some reflected at the Cu surface, an interaction between the microwave field and the charges at the surface induced an electric field. The induced electric charge remained significant at the surface and generated the surface current (I_e), causing a localized overheating in the form of conduction loss at the Cu surface as shown in Figure 3.5.

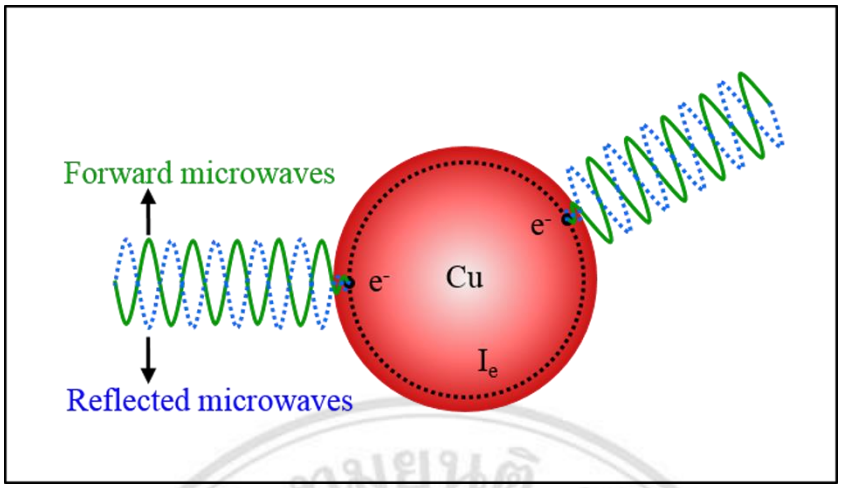

Figure 3.5 Some parts of microwaves are absorbed by Cu and some parts are reflected leading to a localized overheating and power loss at the Cu surface.

The power lost (P) per unit area of surface during the interaction of microwave-Cu particles can be written as follows [95]

$$P_{conduction\ loss} = \frac{2R_S \left|E_0\right|^2}{\eta_0^2}, \qquad (3.6)$$ where

R_S is surface resistivity ($R_S = \frac{1}{\sigma d}$), E_0 is electric field amplitude at the surface, and η_0 is the impedance of free space.

3.2 Plasma Phenomena

The localized heating as it exists, on average, at the Cu surface, leads to little melting at the surface. This means, the rotated charges, which are confined to the surface due to the heating, were able to migrate and rearrange in order for the charged particles to remain quasineutral. High electric fields in a microwave produce remarkably different voltages between the one tip to its neighbor tip of opposite charged particles. This special case can lead electrons passing through the neighbor tip gap toward one of the tips. Then, air breakdown in high electric fields occurred and generated plasma containing copper ions [98]. Next, the plasma sputtered around the Cu particles as shown in Figure 3.6 (a, b and c).

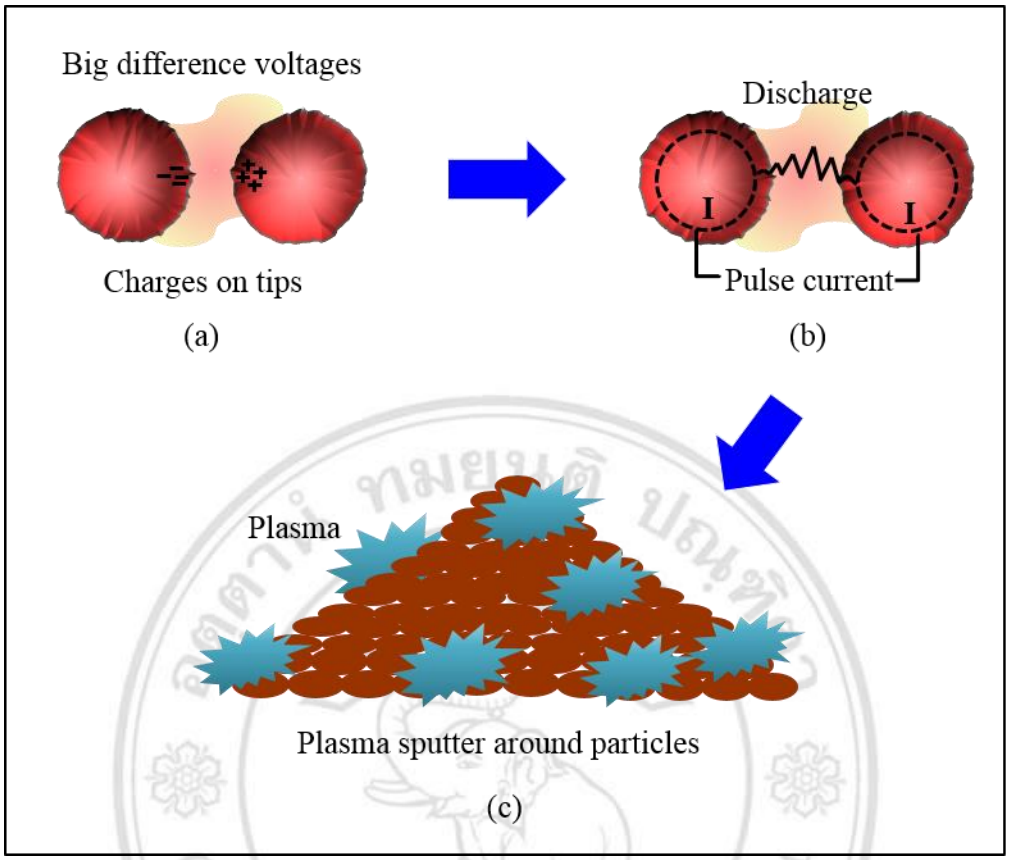

Figure 3.6 Schematic of microwave – Cu particle interactions, (a) remarkably different voltages between the tips occurred, (b) electrons passing through the gap between the tips, and (c) plasma sputter around the Cu particles.

Meanwhile, the electric discharge produced pulse current on the particle surface and the current caused the surface to heat up more quickly. This generated rapid evaporation, melting and neck connection areas between the Cu particles [99].

3.3 Nucleation

After the plasma and evaporation formed, the copper ions reacted with oxygen ions inside the microwave to form the initial phase of Cu_2O thin film. Consequently, the CuO is formed as a result of oxygen passing through hot Cu_2O to oxidize to CuO as follows.[100, 101]

$$4Cu + 2O \dashrightarrow 2Cu_2O \quad (3.7)$$

$$2Cu_2O + 2O \dashrightarrow 4CuO. \quad (3.8)$$

Owing to the rapid increase of copper oxide vapor, it resulted in a higher vapor pressure of copper oxides than its normal environment (i.e., copper oxide under normal conditions in air). The high vapor pressure is called “supersaturation vapor pressure”. At extremely high vapor supersaturation, condensation took place and microscopic droplets formed. This phenomenon is called “condensation nuclei”. If the nuclei become larger than the critical nucleation size (r_c), they will overcome a free energy barrier to form nuclei and continue to grow. For simplicity, r is a nucleus radius nucleating within the bulk. The total free energy of the system is ΔG, which is based on vapor condensation to crystallize and referred to as Gibbs equation. This equation divided into bulk quantity and surface quantity as follows

$$\Delta G = 4\pi r^2 \gamma + \frac{4}{3}\pi r^3 \Delta G_V, \tag{3.9}$$

and

$$\Delta G_V = \frac{-k_B T}{\Omega} \ln\left(\frac{P_V}{P_S}\right), \tag{3.10}$$

where ΔG_V is free energy change per unit volume of solid from the liquid, γ is free energy change per unit area of surface, k_B is the Boltzmann constant, T is temperature in the system, P_V is the pressure of supersaturated vapor, P_s is equilibrium vapor pressure, and Ω is atomic volume. The alternate form of ΔG_V can be written as:

$$\Delta G_V = \frac{-k_B T}{\Omega} \ln(1+S), \tag{3.11}$$

where S is the supersaturation defined by: $S = (P_V - P_S)/P_S$. If, $\Delta G_V < 0$ this suggests that $P_V > P_S (S > 1)$ for nucleation to proceed.

For example in spherical homogeneous nucleation, the critical radius, r_c , and the maximum energy barrier of height, ΔG^*, at the critical point $(d\Delta G / dr) = 0$, can be written as

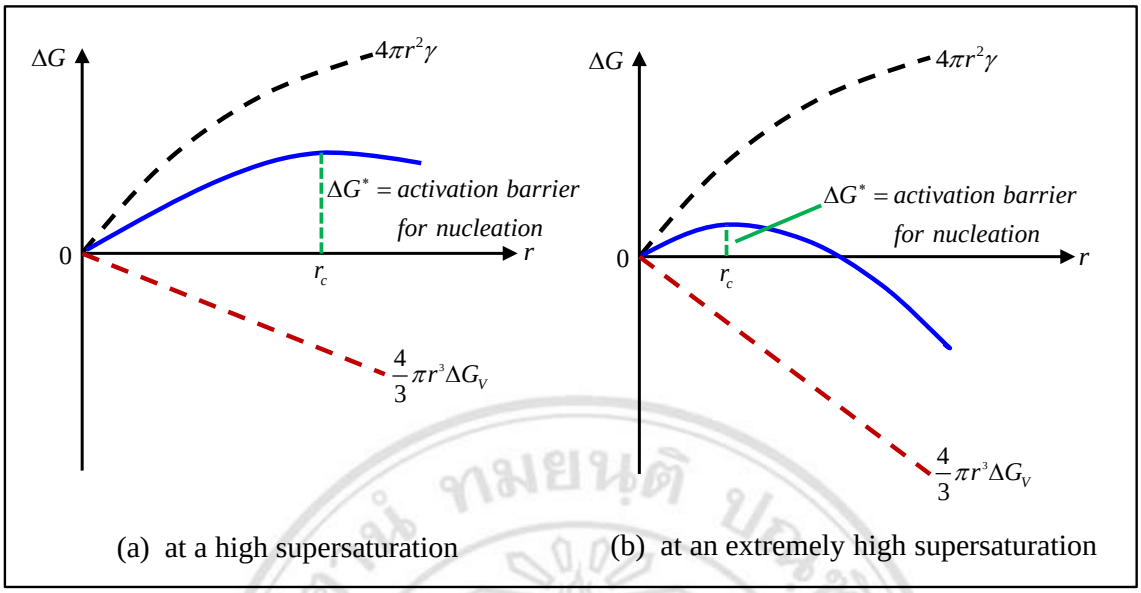

Figure 3.7 Total free energy as a function of nuclei size with degree of supersaturation.

$$r_c = \frac{2\gamma}{\Delta G_V}, \tag{3.12}$$

and

$$\Delta G^* = \frac{16\pi\gamma^3}{3(\Delta G_V)^2}. \tag{3.13}$$

According to Eq.(3.12) and (3.13), the critical radius r_c and the critical free energy ΔG^* depend on the ΔG_V value that itself depends on supersaturation (S) (Deriving physics equations is shown in APPENDIX B). The increase of the supersaturation level (S) leads to a decrease of the barrier for the critical activation energy and the value of the critical size. Finally, the energy becomes so low and nucleation becomes more rapid while the nuclei size gets smaller as shown in Figure 3.7.

3.4 Structure Formation

After the nucleation, the stable nuclei of copper oxide flowed up to the top surface of the quartz rod and formed as a Cu_2O thin film as shown in Figure 3.8. In the continuous process, some of the nuclei deposited at the Cu_2O/ CuO thin films forming Cu_2O/CuO atoms in nanofiber form as shown in Figure 3.9 (a ,b).

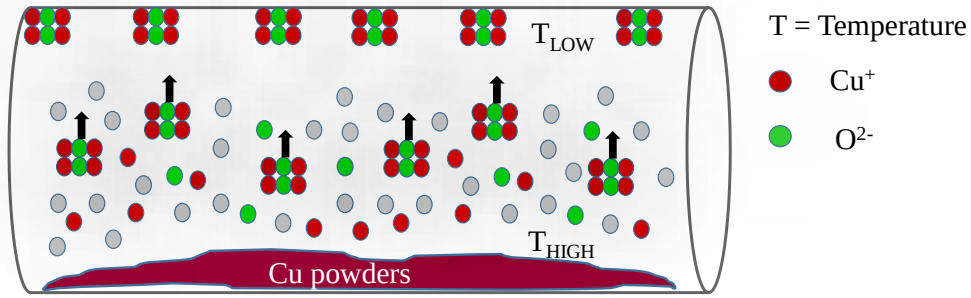

Figure 3.8 The stable nuclei of copper oxide flowed up to the top surface of the quartz rod to form as a Cu_2O thin film

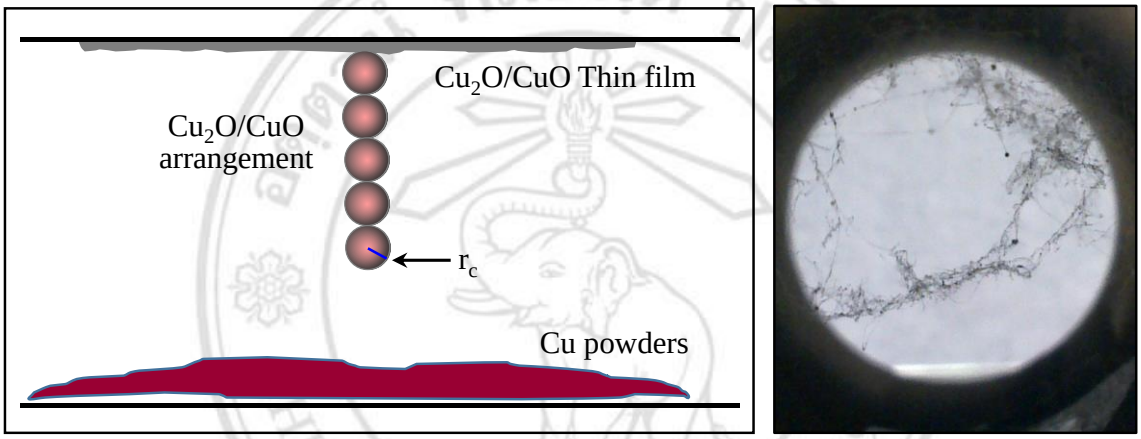

(a) (b)

Figure 3.9 (a) Schematic and (b) real representation of Cu_2O/CuO nanofiber growth inside a quartz tube.

The metal–oxide nuclei arrangement must be self-organized based on minimum total surface energy. The surface of Cu_2O (111) was identified as the lowest-energy surface [102], which is about 0.71 J/m^2 with non-polar [103]. The surface energy (γ) is defined as

$$\gamma = \frac{(Energy\ required\ \ per\ surface\ atom)}{(number\ of\ \ surface\ atom\ /\ surface\ area)} = \frac{\Delta H_S}{2N_A}\left(\frac{N}{A}\right), \qquad (3.14)$$

where ΔH_S is the enthalpy of sublimation, N_A is the number of atom per one-mole crystal, N is the number of surface atom, and A is the surface area.

The shape of a crystal is assigned by considering the surface energies to minimize the total surface free energy of the crystal [104, 105]. Thus, Cu2O (111) surface will be

favored and exposed. However, its lowest energy surface leads to the most stable surface and has minimum velocity of growth [103, 106]. As a result, the growth in Cu_2O (111) surface direction has the lowest speed. Thus, we suggest that crystal growth is preferentially in one orientation, and finally, the crystal forms in a fiber shape. Significantly, the XRD results of the nanofibers in this research (Figure 2.9) correspond to the XRD pattern of Cu_2O nanowires reported in the work of G. Ma et al [107].

Manipulating supersaturation level can influence nucleation and crystal growth resulting in the different morphologies of crystals [108, 109]. Here, ethanol was a parameter, which influenced nucleation and growth stages of copper oxides. It increased supersaturation level as shown in Figure 3.2 and suppressed surface energy in the crystallization process.

Exclusively, the copper oxide nanoparticles were achieved within the first minute of the formation, while the first fibers were obtained after at least 3 min (as shown in Figure 2.3). The quick formation mechanism is clear evidence of the ethanol influence. This had an effect on the nucleation of the copper oxide nanoparticles. Ethanol is a polar solvent with the structural formula C_2H_6O and has a 12.8^oC flash point. Under microwave radiation, electric dipoles of ethanol vibrated rapidly in accordance with the alternating electric field of microwaves and generated a dielectric loss in the form of heat in the system as shown in Figure 3.10 [110].

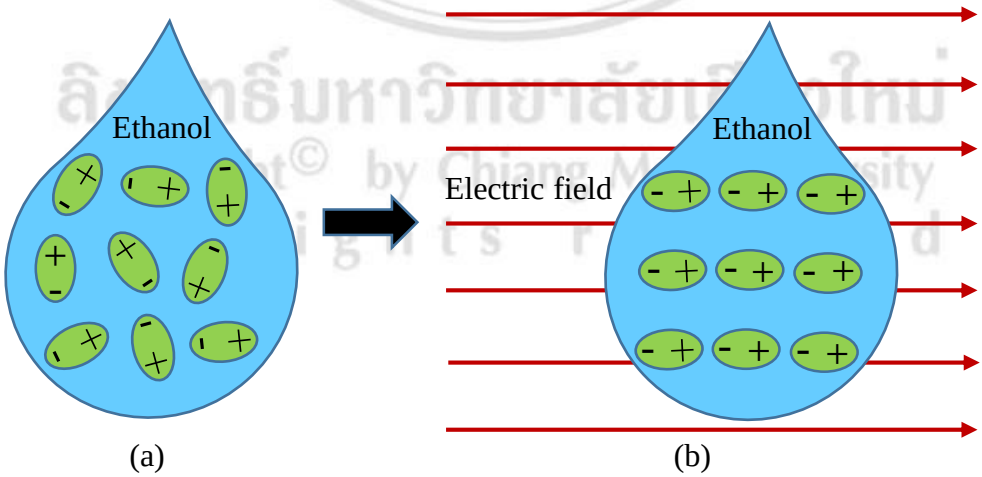

Figure 3.10 Electric dipole arrangements of ethanol (a) before and (b) after putting in electric field of microwaves.

The ability of ethanol to absorb microwave energy and to convert it into heat is represented by the dissipation factor or loss tangent, $\tan\delta$, as seen in the Eq. (3.3). The δ occurs from dipolar reorientation of ethanol in an alternating electric field of microwaves. A comparison of the loss tangent between ethanol and water at a temperature of 20°C and a microwave heating frequency of 2.45 GHz showed that $\tan\delta$ of ethanol, 0.94, was higher than that of water, 0.123 [111]. This indicated that ethanol has a greater ability to dissipate the microwave energy into heat. Thus, the power loss of microwave energy per unit area of surface due to dielectric loss, $P_{dielectric\ loss}$, can be represented as follows [112]

$$P_{dielectric\ loss} = \omega\varepsilon_0\varepsilon'\tan\delta\left|E_0\right|^2. \tag{3.15}$$

Therefore, the total power lost (P_{total}) per unit area of surface during the interaction of microwave-Cu particle-ethanol can be written as follows [112]

$$\begin{aligned} P_{total} &= P_{conduction\ loss} + P_{dielectric\ loss} \\ &= \frac{2R_S\left|E_0\right|^2}{\eta_0^2} + \omega\varepsilon_0\varepsilon'\tan\delta\left|E_0^2\right|. \end{aligned} \tag{3.16}$$

Next, the rapid increase of power lost in the form of heat accelerated the interaction in the system and resulted in an extremely high supersaturation vapor pressure within a very short time. It suggested that the rapid increase of supersaturation level caused a decrease of the surface barrier for the critical activation energy. This led to smaller nuclei size of copper oxides than nuclei size of copper oxides formed by the precursor with no ethanol. In addition, the continuous higher heat being generated and the intensity of the CuO formation phase have been clearly confirmed by the XRD results as a function of the addition of ethanol quantities (as shown in Figure 2.15). The percentages of CuO at Cu+E0.0 (fibers), Cu+E0.2, Cu+E0.3, and Cu+E0.4 were 7.2%, 10.6%, 19.9%, and 47.3%, respectively. The exhibited trend to a higher percentage of CuO confirmed the heat increase and partial conversion of structural composition from Cu_2O to CuO after ethanol addition. We speculated that the reactions for copper powders and ethanol within a punctured microwave, in open-air, can be described according to

$$6Cu + C_2H_6O + 5O_2 \rightarrow 2CuO + 2Cu_2O + 3H_2O + 2CO_2 \quad (3.17)$$

For the crystallization stage, the results of SEM images of nanoparticles in spherical shapes suggests that during nuclei formation, ethanol was absorbed by the nuclei surfaces. The ethanol absorption on specific crystal planes of copper oxide surfaces might have an effect on Cu^{2+} ions. This could effectively reduce the potential of Cu^{2+} ions for electro crystallization [113]. Then, ethanol reduced the energy barrier of the nuclei and contributed to the decrease of the surface energy of Cu_2O/CuO. After critical nuclei formation and acceleration of the crystallization pathways, this results in formation of spherical nanoparticles with minimum surface energy [114, 115].

The quantity of ethanol was an important factor affecting the nanoparticle sizes. At 0.2 mL of ethanol, the number of nanoparticles, which have diameters more than 120 nm, was greater than 34%. Whereas, at 0.3 mL, only 25% of the nanoparticles was larger than 120 nm. The results could suggest that an ethanol quantity of 0.3 mL can generate a higher supersaturation and a lower energy at the crystal face as compared to a quantity of 0.2 mL [116]. Thus, 0.3 mL of ethanol addition in 1 g of copper powders forced copper oxide formation to a more homogeneous size in the spherical shape, 80-120 nm. Although, the formation mechanism in a rough sheet of copper oxide is still unclear, the results indicated that more ethanol, 0.4 mL, increased the supersaturated vapor to a very high pressure leading too much of nucleus formation. Then, each nucleus was squeezed together because of the high pressure and, finally, the rough sheet occurred.

3.5 Chapter Summary

Pure copper powder-ethanol (C_2H_6O) interactions have led to the transformation of copper oxide nanofibers to nanoparticles in few minutes under microwave irradiation. The transformation can be attributed to surface reactions of ethanol in polar characteristic way that accumulated thermal into Cu powders. The polar solvent of the ethanol had an influence on the transformation mechanism by enhancement heating up by rapid vibration with electric field of microwave causing a high supersaturated vapor in the system and a speedy arrangement of nuclei. Then, the ethanol reduced surface energy of the copper oxides during self-organization and accelerated crystallization process to form copper oxide nanoparticles with comprising CuO/Cu_2O in spherical shape. Due to the morphologies and physical properties of both copper oxide nanostructures, they are expected to use in ZnO DSSCs for efficiency enhancement as follow the information in chapter 4.